CHEMISTRY OF MATERIALS

Article

pubs.acs.org/cm

Chemical Vapor Deposition of GaP and GaAs Thin Films From [^{n}Bu$_2$Ga(μ-E^{t}Bu$_2$)$_2$Ga^{n}Bu$_2$] (*E* = P or As) and Ga(P^{t}Bu$_2$)$_3$

Fei Cheng,[†] Kathryn George,[†] Andrew L. Hector,[†] Marek Jura,[‡] Anna Kroner,[§] William Levason,[†] John Nesbitt,[#] Gillian Reid,*[,†] David C. Smith,*[,#] and James W. Wilson[#]

[†]School of Chemistry, University of Southampton, Southampton SO17 1BJ, U.K.

[‡]ISIS, STFC, Harwell Innovation Campus, Didcot, Oxfordshire, OX11 0QX, U.K.

[§]Diamond Light Source plc, Harwell Innovation Campus, Didcot, Oxfordshire OX11 0DE, U.K.

[#]School of Physics and Astronomy, University of Southampton, Southampton SO17 1BJ, U.K.

Supporting Information

ABSTRACT: Low pressure chemical vapor deposition (LPCVD) using the single-source precursors [^{n}Bu$_2$Ga(μ-E^{t}Bu$_2$)$_2$Ga^{n}Bu$_2$] (E = P or As) in the temperature range 723−823 K (0.05 mmHg), gives shiny yellow or silvery gray films of GaP and GaAs, respectively, on silica. The composition and morphology of the deposited materials have been probed via X-ray diffraction (XRD), scanning electron microscopy/energy-dispersive X-ray (SEM/EDX), X-ray photoelectron spectroscopy (XPS), atomic force microscopy (AFM), and Raman spectroscopy, revealing crystalline (cubic) GaE with 1:1 Ga/E ratios. The GaP forms nanorods growing perpendicular to the substrate surface and is rougher than the GaAs, which appears to form smaller, densely packed microcrystallites. While the GaAs films produced in this way did not exhibit any significant luminescence, the reflective GaP films obtained by LPCVD were of good electronic quality, revealing photoluminescence comparable to that of a single crystalline GaP reference. LPCVD using Ga(P^{t}Bu$_2$)$_3$ gives GaP, although this appears to be an inferior reagent compared to the dimer. Unlike the corresponding [^{n}Bu$_2$In(μ-E^{t}Bu$_2$)$_2$In^{n}Bu$_2$] dimers (see Aksomaityte et al., *Chem. Mater.* **2010**, *22*, 4246) which gave InE films and nanowires from supercritical chemical fluid deposition in sc-CO$_2$/hexane, under the same conditions (773 K, 12 MPa), the gallium dimer precursors mostly failed to give GaE. Instead significant carbon deposition occurred, indicating solvent degradation.

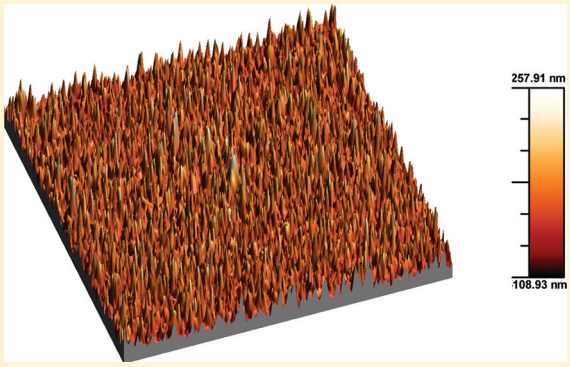

KEYWORDS: *gallium phosphide, gallium arsenide, chemical vapor deposition, luminescence*

1. INTRODUCTION

Semiconductors composed of group 13 and 15 elements (III−V materials) have huge technological significance, particularly for optoelectronic applications.[1] A key application for GaP is low cost green, orange, and red light emitting diodes, which have been produced commercially since the 1970s. GaAs is used in laser diodes and high efficiency solar cells and is also a valuable alternative to silicon for applications that require higher electron mobility, thermal stability, and resistance to radiation damage. In addition, GaAs and GaP based alloys are used in a wide range of III−V heterostructured devices.

Key deposition methods for III−V materials are vapor phase epitaxy, molecular beam epitaxy and metal−organic chemical vapor deposition (MOCVD), which have been refined to the extent that they are capable of producing high purity material with good control of film thickness. Trimethylgallium in conjunction with phosphine (PH_3) or arsine (AsH_3) have dominated CVD deposition of GaP and GaAs since the pioneering work of Manasevit and Simpson.[2] Other volatile liquid reagents, such as ^{t}BuEH$_2$, have been employed in place of the extremely toxic EH_3 gases in dual-source CVD, giving better control of composition (particularly for GaP), although these are still pyrophoric.[3] While nanowires of GaP and GaAs have been grown using ^{t}Bu$_3$Ga and E(SiMe$_3$)$_3$ (E = P or As) seeded with thiol-stabilized gold nanocrystals in supercritical hexane,[4] this is a rare example of dual-source deposition from such media. It is acknowledged that the reagents typically used in the dual-source deposition of GaE are not readily amenable to other types of deposition which may be necessary for certain applications, such as in nanoparticle formation (via high temperature solvents) or for filling high aspect ratio pores (via supercritical chemical fluid deposition (SCFD)). Single-source precursors are attractive as alternatives, as they tend to be powdered solids, rather less toxic or pyrophoric, and hence, if GaE with sufficiently high purity can be obtained, these may be much more convenient for certain applications and

Received: July 27, 2011
Revised: September 23, 2011
Published: November 15, 2011

deposition media. Previous work shows that adducts of $GaClR_2$ with tertiary phosphines or arsines such as EEt_3 generally lack volatility and surface mobility.[5] Using anionic phosphido or arsenido complexes can be advantageous, although the chloro-species $[Cl_2Ga(\mu\text{-}ER_2)]_n$ are unlikely to have sufficient volatility for CVD. $[^nBu_2Ga(\mu\text{-}P(SiMe_3)_2)]_2$ is also insufficiently volatile for CVD, but it may be pyrolyzed readily to give GaP, albeit with significant Si contamination.[6] In previous work, a series of single-source molecular species, such as of the form $[R_2^1Ga(\mu\text{-}ER_2^2)]_n$ (E = P, As; R^1, R^2 = alkyl; n = 2 or 3) or $Ga(AsR_2)_3$, have been used to good effect, and shown to be particularly effective for GaAs deposition, although studies on GaP deposition from these reagents are much more limited in the open literature.[7,8]

In another work we have shown that supercritical chemical fluid deposition (SCFD) may be used to deposit high quality CdS[9] and thin films of luminescent quality InP and InAs nanowires.[10] The III−V materials were produced from the dimeric single-source precursors $[^nBu_2In(\mu\text{-}E^tBu_2)_2In^nBu_2]$ (E = P or As) in single phase sc-CO_2/hexane at 773 K; a key feature being the high solubility of the dimers in the supercritical fluid medium and their relatively high stability compared to the reagents typically used in dual-source deposition, trialkylindium and PH_3 or AsH_3. Notably, low pressure (LP) CVD experiments also using these reagents were much less successful, leading to indium rich phases.

In this paper, we describe our efforts toward deposition of GaP and GaAs under comparable conditions from the corresponding gallium precursors $[^nBu_2Ga(\mu\text{-}E^tBu_2)_2Ga^nBu_2]$ using both LPCVD and SCFD, as well as LPCVD from the tris-phosphido gallium reagent $Ga(P^tBu_2)_3$. The preparations of these precursor compounds have been described by Cowley and co-workers,[11b,c] and they have also shown that the arsenide-reagents, $[R_2Ga(\mu\text{-}As^tBu_2)_2GaR_2]$ (R = Me, ^{i}Pr, ^{t}Bu), may be used to grow n- (Me) or p-type (^{i}Pr, ^{t}Bu) GaAs by LPCVD, including epitaxial films.[8,11] In practice, $Ga(As^tBu_2)_3$ seemed to give the highest quality GaAs, attributed in part to the absence of Ga−C bonds in the precursor.[11a] In contrast, deposition of GaP films using the molecular, single-source phosphido-reagents has been much less studied. Given our successful deposition of InE from $[^nBu_2In(\mu\text{-}E^tBu_2)_2In^nBu_2]$ via SCFD, we have now undertaken similar studies on Ga reagents using both deposition techniques, demonstrating here that while in practice the $[^nBu_2Ga(\mu\text{-}E^tBu_2)_2Ga^nBu_2]$ precursors are not well-suited to SCFD, the phosphido-species does appear to be a valuable reagent for CVD of GaP.

2. EXPERIMENTAL SECTION

All reactions were conducted using Schlenk, vacuum line, and glovebox techniques, under a dry nitrogen atmosphere. The reagents were stored and manipulated using a glovebox. $[^nBu_2Ga(E^tBu_2)_2Ga^nBu_2]$ (E = P, As) and $Ga(P^tBu_2)_3$ were prepared by the methods published by Cowley et al.[11b,c] Hexane, toluene, diethyl ether, and THF were dried by distillation over sodium/benzophenone. $GaCl_3$, ^{n}BuLi, ^{t}BuLi, $AsCl_3$ and HP^tBu_2 were obtained from Aldrich and used as received. LiP^tBu_2, HAs^tBu_2 and $LiAs^tBu_2$ were prepared according to the method of Holga et al.[12]

2.1. Characterization. X-ray diffraction (XRD) analysis was performed on a Bruker AXS D8 Discover with GADDS detector using Cu $K\alpha_1$ radiation and a 5° incident angle. Scanning electron microscopy (SEM) was performed on gold coated samples at an accelerating voltage of 20 kV using a JEOL JSM 5910, and energy-dispersive X-ray (EDX) data on carbon coated samples were obtained with an Oxford INCA300 detector. Raman measurements were taken at an excitation energy of 3.09 eV, which was produced by a Coherent Inc. mode locked Mira 900 Ti:Sapphire laser and second harmonic generator (SHG). The bandwidth of the pulses was 0.30 nm; the pulses were produced at a repetition rate of 80 MHz. The Raman microscope was set up in a colinear alignment, where an Olympus LMPlan 50× IR objective was used to focus an 8 mW beam to a spot size ≈ 1 μm^2 on the sample and subsequently collect the scattered Raman light. The Raman signal was detected with a Princeton Instruments Pi-Action TriVista triple spectrometer fitted with a Roper Scientific ST133B nitrogen cooled charge-coupled device (CCD). Photoluminescence measurements were made with a 405 nm excitation from a Diode laser (Sanyo, DL-3146-151). A power density of 8.7 W cm^{-2} was used. The emission was collected and collimated by 0.25 NA lens, passed through a 45° laser line mirror (CVI TLM1-400-45P-2037) to remove the intense laser light, and then focused into an optical fiber and analyzed using a UV−visible spectrometer (Ocean Optics, HR4000). The throughput of the system was corrected for using a fiber coupled tungsten−halogen white light source placed at the position of the sample. Atomic force microscopy (AFM) was conducted using a Veeco Dimension 3100 in tapping mode. Absorption spectra were recorded using the diffuse reflectance attachment of a Perkin-Elmer Lambda 19 spectrometer.

X-ray photoelectron spectroscopy (XPS) data were obtained using a Scienta ESCA300 photoelectron spectrometer with a rotating anode Al $K\alpha$ ($h\nu$ = 1486.7 eV) X-ray source at the National Centre for Electron Spectroscopy and Surface Analysis (NCESS), Daresbury Laboratory, U.K. Samples were etched using argon ion bombardment for 300 s at 3 keV. Where necessary, sample charging was eliminated by use of an electron flood gun delivering 5 eV electrons. The Ga 2p and 3p, As 2p and 3p, P 2s and 2p, C 1s, and O 1s spectra were collected. The CasaXPS package was used for data analysis. Data were referenced to the C 1s peak, which was assigned a binding energy of 284.8 eV.

2.2. LPCVD from $[^nBu_2Ga(E^tBu_2)_2Ga^nBu_2]$ (E = P, As). In a typical experiment, 0.100 g of reagent and silica substrates were loaded into a closed-end silica tube in a glovebox (precursor at the closed end, followed by substrates positioned end-to-end through the heated region). The tube was set in a furnace such that the precursor was outside the heated zone, the tube was evacuated, then heated to the target deposition temperature (773 K) under 0.05 mmHg (66 Pa) and the furnace was allowed to stabilize. The tube position was then adjusted so that the precursor was moved gradually toward the hot zone until slow sublimation was observed (approximately 573 K based on temperature profiling carried out after deposition). At this point the sample position was maintained until sublimation and deposition were complete. The tube was then cooled to room temperature and transferred to the glovebox where the tiles were removed and stored under an N_2 atmosphere prior to analysis. Typically, the best films were found just outside the furnace hot zone and 50−100 mm from the precursor, where the temperature was ca. 30 K below the set temperature, and these were the films selected for further study. Similar experiments were conducted at 623, 673, 723, and 823 K.

2.3. LPCVD from $Ga(P^tBu_2)_3$. In a typical experiment, 0.100 g of reagent and silica substrates were loaded into a quartz tube in a glovebox. The tube was set in a furnace and evacuated; then, it was heated to achieve deposition at 773 K under 0.05 mmHg (66 Pa), using the method described above.

Samples deposited at lower temperatures tended to have a more matte appearance, whereas higher temperatures gave reflective films, and EDX measurements revealed Ga:E ratios closer to 1:1 from the higher temperature depositions. GaAs films obtained were gray, shiny, and reflective, with powdery regions on the substrates closest to the precursor. The majority of the GaP films were yellow or grayish and powdery; however, films deposited at higher temperatures (773 K) were yellow, shiny, and reflective, and these were the ones subjected to more detailed analysis, including photoluminescence measurements. Samples were generally very well adhered to the tiles, as evidenced by the fact they remained intact even when removed from an SEM stub to which they had been attached by carbon tape. Excellent reproducibility was obtained and films were visually very similar between depositions

dx.doi.org/10.1021/cm202158a | Chem. Mater. 2011, 23, 5217−5222

conducted at the same temperature. Similar characterization data were obtained from several different samples.

3. RESULTS AND DISCUSSION

The air-sensitive, white dimeric compounds [^{n}Bu$_2$Ga(μ-E^{t}Bu$_2$)$_2$Ga^{n}Bu$_2$] (E = P or As) were obtained in good yield using the method developed by Cowley and co-workers.[11b,c] The tris-phosphido gallium reagent, Ga(P^{t}Bu$_2$)$_3$, was isolated as an extremely moisture and oxygen sensitive red solid by reaction of GaCl$_3$ with LiP^{t}Bu$_2$ in THF.[11b,c] The solids were stored and manipulated in an N$_2$ purged, dry (<1 ppm H$_2$O) glovebox and were characterized by ^{1}H and ^{31}P{^{1}H} NMR spectroscopy and microanalysis as appropriate.

3.1. LPCVD of GaP and GaAs. LPCVD from [^{n}Bu$_2$Ga(μ-E^{t}Bu$_2$)$_2$Ga^{n}Bu$_2$] was undertaken as described previously[8] at a range of temperatures (50 degree intervals) between 623 and 823 K, leading to clean sublimation of the precursor compound (no residue) and deposition of yellow films (E = P) and shiny silvery films (E = As) onto the silica substrate. The tiles closest to the precursor tended to produce a powdery deposit, whereas in the hotter region of the furnace much more reflective films were produced, and in general, the arsenide reagents yielded more reflective deposits than the phosphide reagent. The films that were selected for further characterization were typically those deposited at approximately at 723 K. These films were selected by visual inspection, choosing either yellow films (E = P) or shiny silvery films (E = As).

By analogy with the GaAs work,[11a] we also studied Ga(P^{t}Bu$_2$)$_3$ as a reagent for deposition of GaP via LPCVD under similar conditions. It was anticipated that the increased P/Ga ratio in the precursor might have a favorable effect on the composition of the deposited films and this reagent has been used successfully to make GaP nanoparticles and quantum dots.[13] These experiments resulted in the deposition of thin shiny yellow films on the slides closest to the precursor, and a significant amount of yellow powdery material remained where the reagent had been positioned originally. The films were shown to be crystalline GaP by X-ray diffraction (XRD) and SEM analysis, with EDX showing Ga/P ratios of 1:1.0. There was some minor variation in composition across the tiles ($< \pm$ 0.1 in ratio of Ga/P by EDX). The remaining yellow powder also contained mainly GaP, along with GaPO$_4$ and other impurities. On the basis that a significant amount of GaP was produced where the precursor complex had been positioned originally, indicating that the sublimation and deposition temperatures for this reagent are very similar, it was concluded that this was an inferior reagent for LPCVD of GaP, and therefore, the discussion below focuses on the materials deposited from the dimeric reagents [^{n}Bu$_2$Ga(μ-E^{t}Bu$_2$)$_2$Ga^{n}Bu$_2$].

XRD measurements on the materials deposited from [^{n}Bu$_2$Ga(μ-E^{t}Bu$_2$)$_2$Ga^{n}Bu$_2$] at 773 K confirmed them to be cubic GaP (a = 5.465(4) − 5.503(9) Å) (Figure 1) and cubic GaAs (a = 5.465(4) − 5.496(5) Å) (Figure 2), respectively (literature values for bulk GaP and GaAs are 5.358 − 5.473 Å and 5.508 − 5.750 Å),[14] with no evidence of other phases. There is no significant variation with temperature and no evidence from the X-ray patterns for preferred orientation of the crystallites.

Raman spectra recorded from the same thin film samples each show two bands (Figure 3), GaP (at 367 and 402 cm^{-1}) and GaAs (at 270 and 291 cm^{-1}), which are entirely in agreement with literature values for the TO and LO phonons in each material, respectively.[15,16] Raman measurements taken at several locations on the sample showed variations in the relative amplitudes of the TO and LO peaks, as well as small shifts in the peak frequencies, which can easily be explained by the microcrystallinity of the sample.

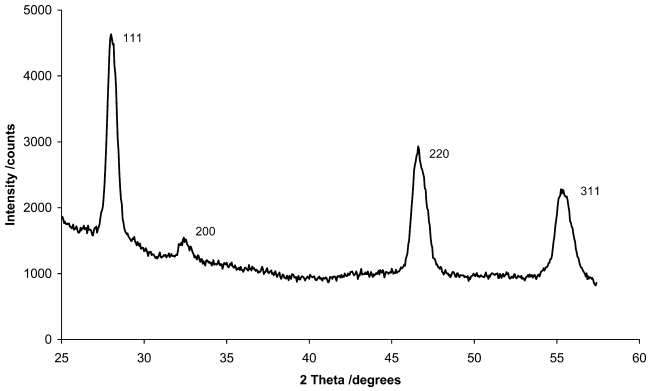

Figure 1. XRD pattern obtained from a GaP thin film grown on silica at 773 K by LPCVD from [^{n}Bu$_2$Ga(μ-P^{t}Bu$_2$)$_2$Ga^{n}Bu$_2$].

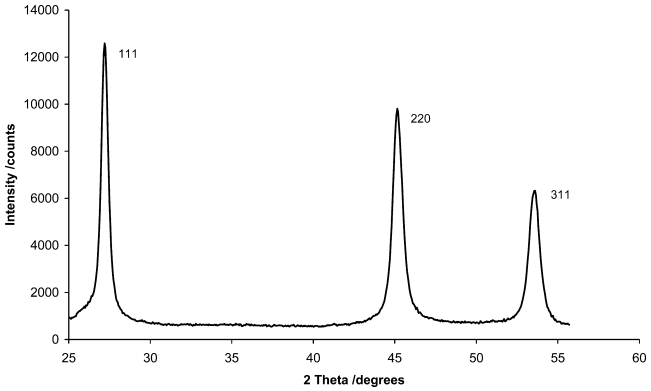

Figure 2. XRD pattern obtained from a GaAs thin film grown on silica at 773 K by LPCVD from [^{n}Bu$_2$Ga(μ-As^{t}Bu$_2$)$_2$Ga^{n}Bu$_2$].

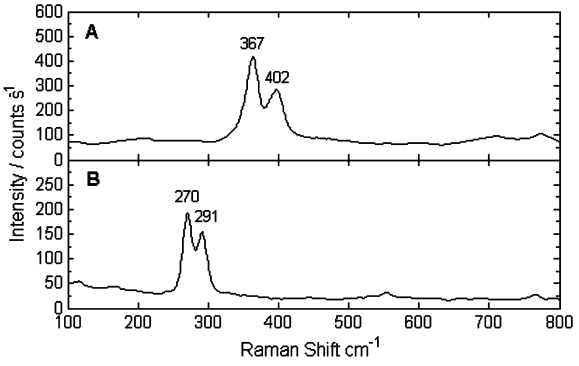

Figure 3. Raman spectra of GaP (a) and GaAs (b) thin films grown by LPCVD at 773 K from [^{n}Bu$_2$Ga(μ-E^{t}Bu$_2$)$_2$Ga^{n}Bu$_2$].

SEM analysis on the more reflective GaP films showed a regular morphology formed of a dense mat of columnar nanorods with a growth direction approximately perpendicular to the substrate surface (Figure 4), and typical GaP films grown at 773 K using 0.10 g of precursor were ~1 μm thick. The GaAs film morphology was much denser and smoother than that of the GaP (Figure 4). AFM measurements (Figure 5) were consistent with the SEM data, revealing that the GaP film surfaces are considerably rougher than the GaAs films produced

dx.doi.org/10.1021/cm202158a | Chem. Mater. 2011, 23, 5217–5222

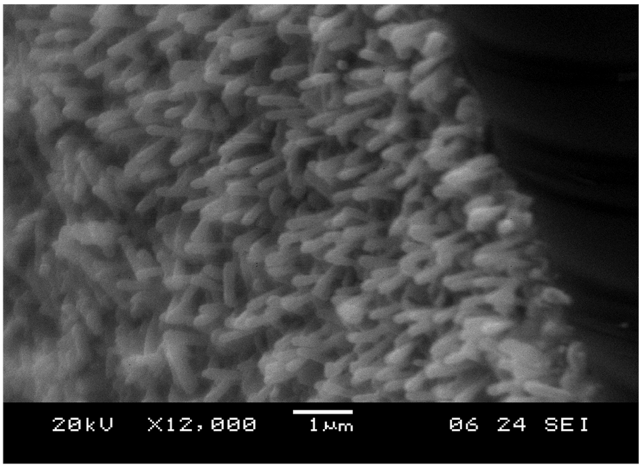

(a)

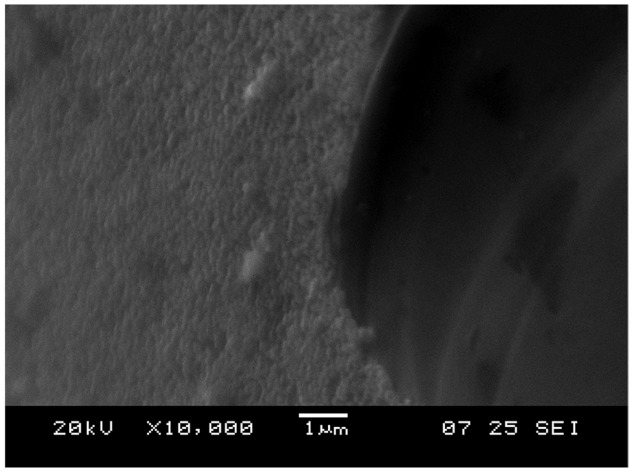

(b)

Figure 4. SEM cross-sectional images of (a) cubic GaP film and (b) GaAs films deposited on silica at 773 K by LPCVD from [$^{n}Bu_2Ga(\mu$-$E^{t}Bu_2)_2Ga^{n}Bu_2$]. Tiles were fractured through the films and the darker regions on the right-hand side of the images are the fractured tile edges.

under the same experimental conditions (GaAs rms roughness = 8.0 nm (2 × 2 μm scan)). The obvious columnar morphology of the GaP surface precluded accurate determination of its rms roughness.

The elemental composition of these deposited materials was probed by EDX analysis, which showed Ga/P and Ga/As ratios closest to 1:1.0 for samples deposited at higher temperature (773 K; see the Supporting Information). XPS measurements on unetched films showed P- or As-deficient compositions. Only one Ga, P, and As environment was observed in these GaE films. For GaAs, both O (15.9 wt %) and C (4.6 wt %) were also evident. With the expectation that the oxygen presence and the pnictogen deficiency were due to reactions of the surface with air (XPS only samples the top few nm of the sample), the samples were Ar ion etched. This resulted in significant reductions in the oxygen and carbon signals (to 10% and 1.8 wt %, respectively). The rod-like morphology of the GaP samples is likely to lead to inherently higher C and O levels pre-etching, as observed, and this also precluded effective etching of the whole of their surfaces; hence, the % C and % O

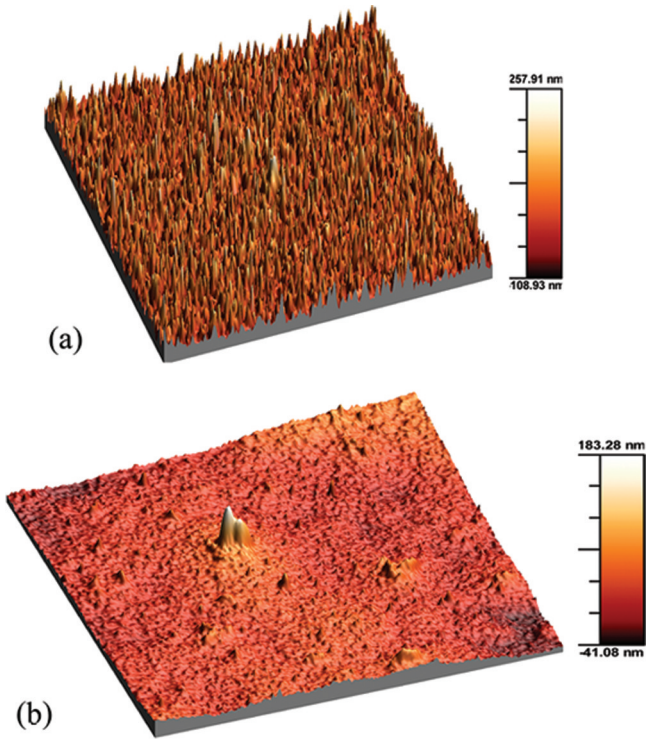

Figure 5. 3-D AFM images (20 μm × 20 μm) of films grown at 773 K by LPCVD from [$^{n}Bu_2Ga(\mu$-$E^{t}Bu_2)_2Ga^{n}Bu_2$], E = P (a) and E = As (b).

determinations from the GaP samples were not possible by XPS.

To probe the electronic quality of the GaP films, photoluminescence measurements were also undertaken on a number of the GaP and GaAs thin film samples. The GaP samples gave photoluminescence whose magnitude and form was comparable with that from a single crystalline sample (99.99%, Aldrich) (Figure 6), suggesting the deposited material has good

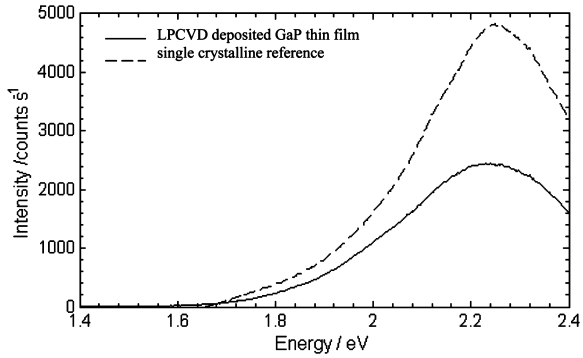

Figure 6. Luminescence spectrum of GaP film grown at 773 K by LPCVD from [$^{n}Bu_2Ga(\mu$-$P^{t}Bu_2)_2Ga^{n}Bu_2$].

electronic quality. However, the GaAs samples gave no measurable luminescence. One likely explanation for this is that the GaAs is formed from nanocrystallites whose surfaces act as nonradiative recombination sites. For this reason we repeated the photoluminescence measurements with samples that had been freshly etched with 12 mol dm^{-3} HCl (for GaAs) or 12 mol dm^{-3} H_2SO_4 (for GaP) for 6 and 10 s, respectively, to try to remove the nonradiative recombination sites.[17,18] The

dx.doi.org/10.1021/cm202158a | *Chem. Mater.* 2011, 23, 5217–5222

etching had little effect for the GaP samples and references. In the case of GaAs, the etching increased the intensity of the luminescence from the single crystal reference by approximately a factor of 6; however, the GaAs samples still produced no luminescence. While this may indicate these samples consist of defective GaAs, it is also possible that the dense nature of the films means that the etchant was unable to reach most of the crystallite interfaces.

An optical transmission measurement from a shiny GaAs film is presented in Figure 7a. While a precise determination of the onset of absorption in the film is difficult, the onset has certainly occurred by 1.46 eV, the accepted band gap of bulk GaAs. This suggests there may be sub-band gap absorption which would agree with the conclusion from the photoluminescence measurements that the GaAs films are not of high optical quality. The GaP films are scattery, and so, for these films, we performed absorbance measurements using an integrating sphere based system. A result from these measurements is shown in Figure 7b. While these measurements do not show a clear onset of absorption at 2.27 eV, the GaP direct band gap E_g, there is a clear feature at approximately 2.78 eV, the GaP zone center band gap E_o. This, combined with the PL measurements that show emission at E_g, leaves no doubt that the optical properties of these films are in agreement with the accepted band structure of GaP.

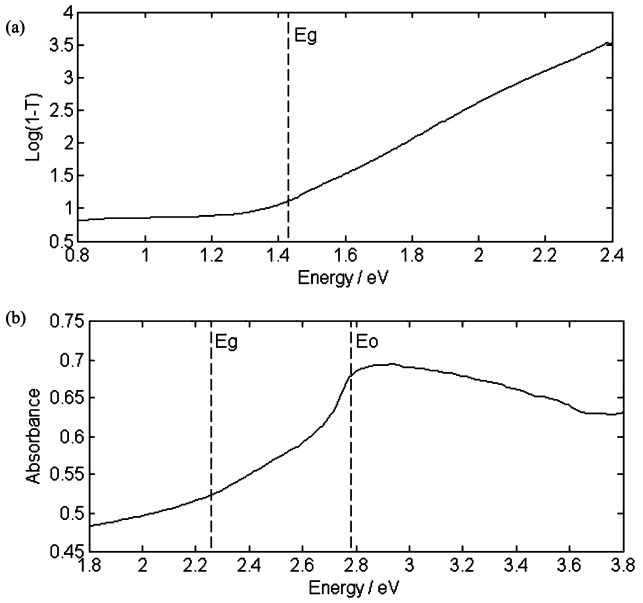

Figure 7. (a) Transmission spectrum of GaAs film grown at 773 K and (b) diffuse reflectance spectrum of GaP film grown at 773 K.

3.2. Attempted SCFD of GaP and GaAs. Our earlier work has demonstrated that reflective films of InP and InAs nanowires, showing good band-edge luminescence in the former case, could be deposited from the analogous [^{n}Bu$_2$In-(μ-E^{t}Bu$_2$)$_2$In^{n}Bu$_2$] precursors by SCFD from single phase sc-CO$_2$/hexane at 773 K (12 MPa).[10] The Ga dimers also exhibit good solubility in hydrocarbons, and hence, similar experiments were performed using these reagents, in an attempt to deposit GaP and GaAs. Under these conditions, shiny green films were often obtained with phosphide and gray, scattering films were obtained with arsenide. However, the films were always amorphous and contained high levels of carbon, with highly variable Ga/P ratios and no As detected by EDX. It has been shown that Lewis acidic metals can promote the decomposition of hydrocarbons to carbon (including multiwalled nanotubes) under supercritical conditions;[19] hence, the solvent was changed to benzene, which has been used in solvothermal conditions at temperatures up to 823 K to produce transition metal nitrides.[20] However, this was also unsuccessful, leading to significant carbon deposits, but not GaP (or GaAs). These results contrast with the successful InE deposition by SCFD, and probably arise as a consequence of the greater reactivity of Ga(III) over In(III) under the supercritical fluid conditions employed. A crystalline film was produced only in one deposition, when a toluene solution of [^{n}Bu$_2$Ga(μ-E^{t}Bu$_2$)$_2$Ga^{n}Bu$_2$] was piped directly into the reactor at 823 K, in very close proximity to the substrate. A small patch of tan-colored, scattering film was found to consist of GaP contaminated with Ga_2O_3.

4. CONCLUSIONS

This work has demonstrated that the [^{n}Bu$_2$Ga(E^{t}Bu$_2$)$_2$Ga^{n}Bu$_2$] (E = P, As) dimers are effective single-source precursors for the deposition of crystalline GaE films via LPCVD, although in practice, unlike the indium analogs, they are not well-suited for SCFD under the experimental conditions employed. This is the reverse of the observations we made previously in the indium systems for which SCFD gave good quality InE films of nanowires.[10] Importantly, while the GaP is produced via LPCVD as nanorods and appears to form a rougher surface than the GaAs, the material is of good electronic quality, revealing band-edge luminescence comparable to single crystalline GaP. This is very encouraging given the relative simplicity of the CVD rig employed, indicating that [^{n}Bu$_2$Ga-(P^{t}Bu$_2$)$_2$Ga^{n}Bu$_2$] may be a viable single-source CVD reagent for GaP deposition and suggesting that, in a fully optimized system, with mass flow control and UHV conditions, even better quality GaP may be obtainable.

■ ASSOCIATED CONTENT

Ⓢ Supporting Information

Representative XRD patterns, SEM images, and EDX data for GaP and GaAs deposited from [^{n}Bu$_2$Ga(E^{t}Bu$_2$)$_2$Ga^{n}Bu$_2$] (E = P, As) by LPCVD at different temperatures. This material is available free of charge via the Internet at http://pubs.acs.org.

■ AUTHOR INFORMATION

Corresponding Authors

*E-mail: G.Reid@soton.ac.uk.
*E-mail: D.C.Smith@soton.ac.uk.

■ ACKNOWLEDGMENTS

We thank RCUK (EP/C006763/1 and EP/H007369/1) and the CMSD at STFC for funding and Dr M. E. Light for assistance with the XRD measurements. We also thank STFC for access to NCESS under RG696 and Bob Bilsborrow, Danny Law, and Ben Gray for assistance with collecting and analyzing the XPS data.

■ REFERENCES

(1) (a) Grant, I. R. In *Group 13 Metals Aluminium, Gallium, Indium, and Thallium*, 1st ed.; Downs, A. J., Ed.; Wiley: London, 1993; (b) Malik, M. A.; O'Brien, P. In *Group 13 Metals Aluminium, Gallium, Indium and Thallium*, 2nd ed;Aldridge, S., Downs, A. J., Eds.; Wiley; London, 2011, p 612.

(2) Manasevit, H. M.; Simpson, W. I. *J. Electrochem. Soc.* **1969**, *116*, 1725.
(3) Malik, M. A.; Afzaal, M.; O'Brien, P. *Chem. Rev.* **2010**, *110*, 4417.
(4) (a) Davidson, F. M.,; Wiacek, R.; Korgel, B. A. *Chem. Mater.* **2005**, *17*, 230. (b) Davidson, F. M.,; Schricker, A. D.; Wiacek, R.; Korgel, B. A. *Adv. Mater.* **2004**, *16*, 647.
(5) Zaouk, A.; Constant, G. *J. Phys. (Paris), Colloq.* **1982**, *43*, C5.
(6) Janik, J. F.; Baldwin, R. A.; Wells, R. L.; Pennington, W. T.; Schimek, G. L.; Rheingold, A. L.; Liable-Sands, L. M. *Organometallics* **1996**, *15*, 5385.
(7) Jones, A. C.; O'Brien, P. *CVD of Compound Semiconductors: Precursor Synthesis, Development, and Applications*; Wiley-VCH: Weinheim, Germany, 1997.
(8) Cowley, A. H.; Jones, R. A. *Angew. Chem., Int. Ed. Engl.* **1989**, *28*, 1208.
(9) Yang., J.; Hyde, J. R.; Wilson, J. W.; Mallik, K.; Sazio, P. J. A.; O'Brien, P.; Malik, M. A.; Afzaal, M.; Nguyen, C. Q.; George, M. W.; Howdle, S. M.; Smith, D. C. *Adv. Mater.* **2009**, *21*, 4115.
(10) Aksomaityte, G.; Cheng, F.; Hector, A. L.; Hyde, J. R.; Levason, W.; Reid, G.; Smith, D. C.; Wilson, J. W.; Zhang, W. *Chem. Mater.* **2010**, *22*, 4246.
(11) (a) Cowley, A. H.; Jones, R. A. *Polyhedron* **1994**, *13*, 1149. (b) Arif, A. M.; Benac, B. L.; Cowley, A. H.; Geerts, R.; Jones, R. A.; Kidd, K. B.; Power, J. M.; Schwab, S. T. *J. Chem. Soc., Chem. Commun.* **1986**, 1543. (c) Arif, A. M.; Benac, B. L.; Cowley, A. H.; Jones, R. A.; Kidd, K. B.; Nunn, C. M. *New J. Chem.* **1988**, *12*, 553. (d) Miller, J. E.; Kidd, K. B.; Cowley, A. H.; Jones, R. A.; Ekerdt, J. G.; Gysling, H. J.; Wernberg, A. A.; Blanton, T. N. *Chem. Mater.* **1990**, *2*, 589. (e) Atwood, D. A.; Atwood, V. O.; Cowley, A. H.; Gobran, H. R.; Jones, R. A. *Organometallics* **1993**, *12*, 3517. (f) Atwood, D. A.; Cowley, A. H.; Harris, P. R.; Jones, R. A.; Koschmieder, S. U.; Nunn, C. M. *J. Organomet. Chem.* **1993**, *449*, 61. (g) Cowley, A. H.; Corbelin, S.; Jones, R. A.; Lagow, R. L.; Nail, J. W. *J. Organomet. Chem.* **1994**, *464*, C1. (h) Lakhotia, V.; Heitzinger, J. M.; Cowley, A. H.; Jones, R. A.; Ekerdt, J. G. *Chem. Mater.* **1994**, *6*, 871.
(12) Holga, K. T.; George, C. *Organometallics* **1990**, *9*, 275.
(13) Green, M; O'Brien, P. *J. Mater. Chem.* **2004**, *14*, 629.
(14) Inorganic Crystal Structure Database (ICSD) Fachinformationszentrum Karlsruhe (FIZ), accessed via the United Kingdom Chemical Database Service Fletcher, D. A.; McMeeking, R. F.; Parkin, D. *J. Chem. Inf. Comput. Sci.* **1996**, *36*, 746.
(15) Fu, L.-T.; Chen, Z.-G.; Zou, J.; Cong, H.-T.; Lu, G.-Q. *J. Appl. Phys.* **2010**, *107*, 124321.
(16) Campos, C. E. M.; Pizani, P. S. *Appl. Surf. Sci.* **2002**, *200*, 111.
(17) Adachi, S; Oe, K. *J. Electrochem. Soc.* **1983**, *130*, 2427.
(18) Tjerkstra, R. W. *Electrochem. Solid-State Lett.* **2006**, *9*, C81−C84.
(19) Smith, D. K.; Lee, D. C.; Korgel, B. A. *Chem. Mater.* **2006**, *18*, 3356.
(20) Mazumder, B.; Chirico, P.; Hector, A. L. *Inorg. Chem.* **2008**, *47*, 9684.